arXiv:0806.2794v1 [astro-ph] 17 Jun 2008

Astrophysical Sources of Stochastic Gravitational-Wave Background

T. Regimbau[1] **and V. Mandic**[2]

[1] UMR ARTEMIS, CNRS, University of Nice Sophia-Antipolis, Observatoire de la Côte d'Azur, BP 429 06304 Nice (France)

[2] School of Physics and Astronomy, University of Minnesota-Twin Cities (USA)

E-mail: regimbau@oca.eu, mandic@physics.umn.edu

Abstract. We review the spectral properties of stochastic backgrounds of astrophysical origin and discuss how they may differ from the primordial contribution by their statistical properties. We show that stochastic searches with the next generation of terrestrial interferometers could put interesting constrains on the physical properties of astrophysical populations, such as the ellipticity and magnetic field of magnetars, or the coalescence rate of compact binaries.

1. Introduction

According to various cosmological scenarios, we are bathed in a stochastic background of gravitational waves, memory of the first instant of the Universe, up to the limits of the Plank era and the Big Bang [1, 2]. In addition to the cosmological background (CGB), an astrophysical contribution (AGB) may have resulted from the superposition of a large number of unresolved sources since the beginning of stellar activity, which can be either short lived burst sources, such as core collapses to neutron stars [3, 4, 5, 6] or black holes [7, 8, 9, 10, 11], phase transition or oscillation modes in young neutron stars [12, 13, 14], the final stage of compact binary mergers [15, 16], or periodic long lived sources, typically pulsars [17, 18], the early inspiral phase of compact binaries [19, 20, 21, 22] or captures by supermassive black holes [23, 24], whose frequency is expected to evolve very slowly compared to the observation time.

The astrophysical contribution is important for at least two reasons: on one hand, it carries information about the star formation history, the mass range of neutron star or black hole progenitors, the statistical properties of populations of compact objects like the ellipticity or the magnetic field of neutron stars, or the rate of compact binary mergers. On the other hand, it can be a foreground for the cosmological background, and it has to be modeled accurately to define the best frequency windows where to search for the cosmological background. The rest of this article will be organized as follows: in Sec. 2, we review the spectral properties of the AGBs; in Sec. 3, we discuss how their statistical properties may differ from those of the cosmological background;

in Sec. 4 we present two simple models, the stochastic background from magnetars and double neutron star coalescences, susceptible of producing a continuous stochastic background in the frequency band of terrestrial interferometers; in Sec. 5 we discuss the constraints one can expect to put on these models and on the source populations with the next generations of detectors. Finally, in Sec. 6 we summarize the results and present our conclusions.

2. The spectral properties

The spectrum of the gravitational stochastic background is usually characterized by the dimensionless parameter:

$$\Omega_{gw}(\nu_o) = \frac{1}{\rho_c}\frac{d\rho_{gw}}{d\ln\nu_o} \tag{1}$$

where ρ_{gw} is the gravitational energy density, ν_o the frequency in the observer frame and $\rho_c = \frac{3H_0^2}{8\pi G}$ the critical energy density needed to close the Universe today. For a stochastic background of astrophysical origin, the energy density is given by:

$$\Omega_{gw}(\nu_o) = \frac{1}{\rho_c c^3}\nu_o F_{\nu_o}(\nu_o) \tag{2}$$

where the integrated flux at the observed frequency ν_o is defined as:

$$F_{\nu_o}(\nu_o) = \int f_{\nu_o}(\nu_o, z)\frac{dR(z)}{dz}dz \tag{3}$$

The spectral properties of a single source located at z are given by the fluence:

$$f_{\nu_o}(\nu_o, z) = \frac{1}{4\pi d_L^2}\frac{dE_{gw}}{d\nu_o}(\nu_o) = \frac{1}{4\pi d_L^2}\frac{dE_{gw}}{d\nu}(\nu_o)(1+z) \tag{4}$$

where $d_L = r(1+z)$ is the distance luminosity, r the proper distance, which depends on the adopted cosmology, $\frac{dE_{gw}}{d\nu}$ the gravitational spectral energy emitted by a single source and $\nu = \nu_o(1+z)$ the frequency in the source frame.

When the gravitational emission occurs shortly after the birth of the progenitor, the event rate can be associated with the progenitor formation rate:

$$\frac{dR(z)}{dz} = \lambda\frac{R_*(z)}{1+z}\frac{dV}{dz}(z) \tag{5}$$

where $R_*(z)$ is the cosmic star formation rate per comoving volume (SFR) expressed in $M_\odot$ Mpc^{-3} yr^{-1} and λ the mass fraction converted into the progenitors, assumed to be the same at all redshifts. The $(1+z)$ term in the denominator corrects the cosmic star formation rate by the time dilatation due to the cosmic expansion. In our calculations, we consider the 737 cosmology [25], with $\Omega_m = 0.3$, $\Omega_\Lambda = 0.7$ and Hubble parameter $H_0 = 70$ km s^{-1} Mpc^{-1} (or equivalently $h_0 = 0.7$), corresponding to the so-called concordant model derived from observations of distant type Ia supernovae [26] and the power spectra of the cosmic microwave background fluctuations [27]. We use the recent SFR of [28] derived from new measurements of the galaxy luminosity function in the UV (SDSS, GALEX, COMBO17) and FIR wavelengths (Spitzer Space

Telescope), which allowed to refine the previous models up to redshift $z \sim 6$, with very tight constraints at redshifts $z < 1$ (and quite accurate up to $z \sim 2$), and normalized by the Super Kamiokande limit on the electron antineutrino flux from past core-collapse supernovas. A parametric fit is given by [28]:

$$R_*(z) = h_0 \frac{0.017 + 0.13z}{1 + (z/3.3)^{5.3}} \tag{6}$$

for an initial mass function (IMF) of the form (modified Salpeter A):

$$\xi(m) \propto \begin{cases} (\frac{m}{m_0})^{-1.5} & \text{for } 0.1 < m < m_0 \\ (\frac{m}{m_0})^{-2.35} & \text{for } m_0 < m < 100 \end{cases} \tag{7}$$

with a turnover below $m_0 = 0.5$ $M_\odot$ and normalized within the mass interval $0.1 - 100$ $M_\odot$ such as $\int m\xi(m)dm = 1$. The element of comoving volume in eq. 5 is given by:

$$\frac{dV}{dz}(z) = 4\pi \frac{c}{H_0} \frac{r(z)^2}{E(\Omega, z)} \tag{8}$$

where $E(\Omega, z) = \sqrt{\Omega_\Lambda + \Omega_m(1+z)^3}$. Combining the expressions above, one obtains:

$$\Omega_{gw}(\nu_o) = \frac{8\pi G}{3c^2 H_0^3} \lambda\nu_o \int_0^{z_{\rm sup}} \frac{R_*(z)}{(1+z)^2 E(\Omega, z)} \frac{dE_{gw}(\nu_o)}{d\nu} dz \tag{9}$$

or replacing the constants G (gravitational constant) and c (speed of light) by their usual values:

$$\Omega_{gw}(\nu_o) = 5.7 \times 10^{-56} (\frac{0.7}{h_0})^2 \lambda\nu_o \int_0^{z_{\rm sup}} \frac{R_*(z)}{(1+z)^2 E(\Omega, z)} \frac{dE_{gw}(\nu_o)}{d\nu} dz \tag{10}$$

where R_* is given for $h_0 = 0.7$. The upper limit of the integral, which depends on both the maximal emission frequency in the source frame and the maximal redshift of the model of star formation history (usually $z_{\rm max} = 5 - 6$), is given by:

$$z_{\rm sup} = \begin{cases} z_{\rm max} & \text{if } \nu_o < \frac{\nu_{\rm max}}{(1+z_{\rm max})} \\ \frac{\nu_{\rm max}}{\nu_o} - 1 & \text{otherwise} \end{cases} \tag{11}$$

Consequently, the shape of the spectrum of any astrophysical background is characterized by a cutoff at the maximal emission frequency and a maximum at a frequency which depends on the shape of both the SFR and the spectral energy density.

3. The detection regimes

Besides the spectral properties, it is important to study the nature of the background. In the case of burst sources the integrated signal received at $z = 0$ from sources up to a redshift z, would show very different statistical behavior depending on whether the duty cycle:

$$D(z) = \int_0^z \bar{\tau}(1+z') \frac{dR}{dz'}(z') dz' \tag{12}$$

defined as the ratio, in the observer frame, of the typical duration of a single event $\bar{\tau}$, to the average time interval between successive events, is smaller or larger than unity.

When the number of sources is large enough for the time interval between events to be small compared to the duration of a single event ($D >> 1$), the waveforms overlap to produce a continuous background. Due to the central limit theorem, such backgrounds obey the Gaussian statistic and are completely determined by their spectral properties. They could be detected by data analysis methods in the frequency domain such as the cross correlation statistic presented in the next section [29]. On the other hand, when the number of sources is small enough for the time interval between events to be long compared to the duration of a single event ($D << 1$), the sources are resolved and may be detected by data analysis techniques in the time domain (or the time frequency domain) such as match filtering [30, 31]. An interesting intermediate case arises when the time interval between events is of the same order of the duration of a single event. These signals, which sound like crackling popcorn, are known as "popcorn noise". The waveforms may overlap but the statistic is not Gaussian anymore so that the amplitude on the detector at a given time is unpredictable. For such signals, data analysis strategies remain to be investigated [32, 33], since the time dependence is important and data analysis techniques in the frequency domain, such as the cross correlation statistic, are not adapted.

4. Models of astrophysical stochastic backgrounds

In this section, we investigate two processes able to produce a continuous stochastic backgrounds in the frequency band of terrestrial interferometers.

4.1. magnetars

Rotating neutron stars (NSs) with a triaxial shape may have a time varying quadrupole moment and hence radiate GWs at twice the rotational frequency. The total spectral gravitational energy emitted by a NS born with a rotational period P_0, and which decelerates through magnetic dipole torques and GW emission, is given by:

$$\frac{dE_{gw}}{d\nu} = K\nu^3(1 + \frac{K}{\pi^2 I_{zz}}\nu^2)^{-1} \text{ with } \nu \in [0 - 2/P_0] \tag{13}$$

where

$$K = \frac{192\pi^4 G I^3}{5c^2 R^6}\frac{\varepsilon^2}{B^2 \sin^2\alpha} \tag{14}$$

In this expression R is the radius of the star, $\varepsilon = (I_{xx} - I_{yy})/I_{zz}$ the ellipticity, I_{ij} the principal moment of inertia , B the magnetic field and α the angle between the rotation and the dipole axis.

In the original scenario of [34, 35], super-strong crustal magnetic fields ($B \simeq 10^{14} - 10^{16}$ G) can be formed by dynamo action in proto neutron stars with very small rotational periods, larger than the break up limit around $0.5-1$ ms, but smaller than the convective overturn at 3 ms. For these highly magnetized neutron stars, the distortion induced by the magnetic torque, becomes significant, overwhelming the deformation due

to the fast rotation. In the case when the internal magnetic field is purely poloidal and matches to the dipolar field B in the exterior, is given by [37]:

$$\varepsilon_B = \beta \frac{R^8 B^2 \sin^2 \alpha}{4GI_{zz}^2} \tag{15}$$

According to the numerical simulations of [37], the distortion parameter β, which depends on both the equation of state (EOS) and the magnetic field geometry, can range between $1 - 10$ for a non-superconducting interior to $100 - 1000$ for a type I superconductor and even take values larger than $1000 - 10000$ for a type II superconductor with counter rotating electric currents. Assuming $R = 10$ km, $I_{zz} = 1.4 \times 10^{45}$ g cm^2, $P_0 = 1$ ms, $\beta = 100$ and the average value given by the observation of SGR and AXP $B = 10^{15}$ G , we obtain $\varepsilon_B \sim 2 \times 10^{-4}$ and $K \sim 3 \times 10^{37}$ erg Hz^{-3}. In this case, the GW emission becomes negligible compared to the magnetic torque and eq. 13 simplifies to

$$\frac{dE_{gw}}{d\nu} \sim K\nu^3 \tag{16}$$

Considering that magnetars represent about 10% of newborn NS, in agreement with the estimates of [36] and population synthesis of [17], we obtain for the mass fraction of the progenitors $\lambda = 0.1\lambda_{NS}$ where the mass fraction of neutron star progenitors is given by:

$$\lambda_{NS} = \int_{8M_\odot}^{40M_\odot} \xi(m) dm = 9 \times 10^{-3} \mathrm{M}_\odot^{-1} \tag{17}$$

where $\xi(m)$ is the modified A Salpeter IMF from eq. 7 and where we have assumed that NS progenitors have masses larger than 8 $\mathrm{M}_\odot$ [28] and that stars with masses larger than 40 $\mathrm{M}_\odot$ give rise to black holes. Evolution of such massive stars being very fast, we can replace the previous expressions in eq. 10, and obtain:

$$\Omega_{gw}(\nu_o) \sim 4 \times 10^{-21} \nu_o^4 \int_0^{z_{\mathrm{sup}}(\nu_o)} dz \frac{R_*(z)(1+z)}{E(z)} \tag{18}$$

The energy density increases as ν_o^4 at low frequencies and reaches a maximum of $\Omega_{gw} \sim 1 \times 10^{-10}$ around 1100 Hz.

When the product βB is large enough ($K >> \pi^2 I \nu^{-2}$), GW emission becomes the most important process. In the saturation regime where the spindown is purely gravitational, eq. 13 simplifies to:

$$\frac{dE_{gw}}{d\nu} \sim \pi^2 I \nu \tag{19}$$

and the energy density increases as ν_o^2 at low frequencies and reaches a maximum of $\Omega_{gw} \sim 1.3 \times 10^{-8}$ around 1600 Hz (Fig. 1). It has been suggested that the internal magnetic field could be dominated by the toroidal component [39, 40]. In this case

$$\varepsilon_B = 1.6 \times 10^{-4} < B_{t,16}^2 > \tag{20}$$

where $< B_{t,16}^2 >$ is the mean value of the internal toroidal component in unit of 10^{16} G, and whether the rotational energy is dissipated due to dipole or GW emission depends on the ratio B_t^2/B.

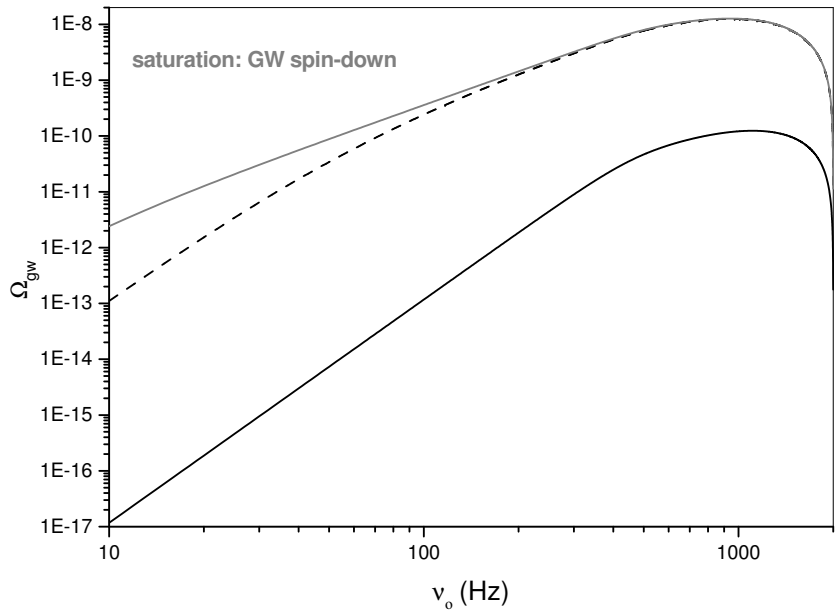

Figure 1. energy density of the background produced by tri-axial rotating magnetars, as a function of the observed frequency, for the canonical model with a poloidal internal magnetic field and ms initial rotational period. The black continuous line corresponds to a model with $B = 10^{15}$ G and $g = 100$ (magnetic spindown regime), the grey continuous line to the purely gravitational spindown regime and the black dashed line to an intermediate case with $B = 10^{16}$ G and $g = 1000$.

4.2. Double neutron star coalescence

The merger of two neutron stars, two black holes or a neutron star and a black hole are among the most important sources of gravitational waves, due to the huge energy released in the process. In particular, double neutron stars (DNSs) may radiate about 10^{53} erg in the last seconds of their inspiral trajectory. In a recent work, [15, 16] used Monte Carlo simulations to calculate the contribution of DNSs to the stochastic background, in the frequency band of ground based interferometers, which corresponds to the last ~ 1000 s before the last stable orbit, when more than 96% of the gravitational energy is released. At that time, the system has been circularized through GW emission and the spectral energy density is given in the quadrupolar approximation by:

$$\frac{dE_{gw}}{d\nu} = K_b \nu^{-1/3} \text{ with } \nu \in [10 - \nu_{LSO}] \tag{21}$$

where

$$K_b = \frac{(G\pi)^{2/3}}{3} \frac{m_1 m_2}{(m_1 + m_2)^{1/3}} \tag{22}$$

For double neutron stars with masses $m_1 = m_2 = 1.4$ M$_\odot$, one obtains $K_b = 5.2 \times 10^{50}$ erg Hz$^{-2/3}$ and the gravitational frequency at the last stable orbit is assumed to be

$\nu_{LSO} = 1.57$ kHz [41].

The merging occurring long after the formation of the system of massive stars, the coalescence rate per unit of comoving volume, which will replace $R_*(z)$ in eq. 5 and eq. 10 is given by:

$$R_c(z) = \int \frac{1+z}{1+z_f} R_*(t_c(z) - t_d) P(t_d) dt_d \tag{23}$$

where z_f is the redshift of formation of the progenitors and $t_c(z)$ the cosmic time at the redshift of coalescence z. The probability distribution of the delay time is usually parameterized by [42, 43, 44]:

$$P_d(t_d) \propto \frac{1}{t_d} \text{ with } t_d > \tau_0 \tag{24}$$

where the minimal delay time $\tau_0 \simeq 20Myr$ corresponds roughly to the time it takes for massive binaries to evolve into two neutron stars [45]. The mass fraction converted into the progenitors is given by the product $\lambda_b = \beta_{NS} f_b \lambda_{NS}$, where β_{NS} is the fraction of binaries which remains bounded after the second supernova event, f_b the fraction of massive binaries formed among all stars and λ_{NS} the mass fraction of NS progenitors. In our reference model we assume $\beta_{NS} f_b = 0.03$ [42]. The merging rate in our galaxy at time t is given by:

$$r_{\rm mw}(t) = \lambda_b \int_{\tau_0}^{t} \rho_{\rm mw}(t - t_d) P_d(t_d) dt_d \tag{25}$$

where $\rho_{mw}(t) = n_{\rm mw}^{-1} R_{mw}(t)$ is the galactic star formation rate in $\mathrm{M}_\odot$ yr^{-1}. Using the model of [46] for the star formation history in the disk, namely

$$R_{mw}(t) = 0.056 \frac{t}{4.5} e^{-\frac{t}{4.5}} \ (\mathrm{M}_\odot \mathrm{yr}^{-1} \mathrm{Mpc}^{-3}) \tag{26}$$

where t is in Gyr, and assuming a density of milky-way equivalent galaxies of $n_{\rm mw} = 0.01$ Mpc^{-3}, we find an actual rate of $r^o_{\rm mw} = r_{\rm mw}(13.5) \sim 3 \times 10^{-5}$ yr^{-1}, in agreement with the expectations derived from statistical studies and population synthesis [47, 42, 48]. We find that sources at redshifts $z > 0.5$ contribute to a truly continuous stochastic background, while sources at redshifts $0.25 < z < 0.5$ are responsible for a popcorn noise, with duty cycles of 1 and 0.1 respectively. The energy density

$$\Omega_{gw}(\nu_0) = 8.6 \times 10^{-10} \nu_o^{2/3} \int_0^{z_{\rm sup}} \frac{R_c(z)}{(1+z)^{7/3} E(z)} dz \tag{27}$$

reaches a maximum of $\Omega_{gw} \sim 7 \times 10^{-10}$ around 500 Hz for the continuous contribution and of $\Omega_{gw} \sim 9 \times 10^{-10}$ around 550 Hz for the popcorn background (Fig. 2). The total background, including the nearest sources down to $z \sim 0$ is slightly higher, with a maximum of $\Omega_{gw} \sim 1.2 \times 10^{-9}$ at 600 Hz.

5. Constraints with the next generations of detectors

We now discuss the constraints one can expect to put on some simple models, with the next generations of terrestrial detectors.

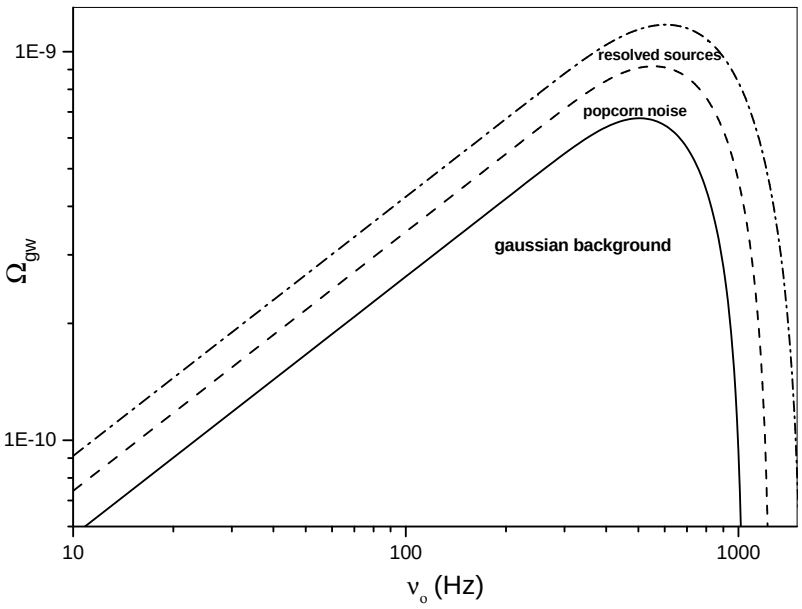

Figure 2. energy density of the continuous background produced by DNS coalescences at $z > 0.5$ (continuous line) and of the popcorn contribution corresponding to sources between $z = 0.25 - 0.5$ (dashed line). The signal from the whole population down to $z = 0$ is also plotted for comparison (dot-dashed line).

5.1. detection

The optimal strategy to search for a stochastic background, which can be confounded with the intrinsic noise background of the instrument, is to cross correlate measurements of multiple detectors. The optimized S/N ratio for an integration time T is given by [29]:

$$(\frac{S}{N})^2 = \frac{9H_0^4}{50\pi^4} T \int_0^\infty df \frac{\gamma^2(f)\Omega_{\rm gw}^2(f)}{f^6 P_1(f) P_2(f)} \tag{28}$$

where $P_1(f)$ and $P_2(f)$ are the power spectral noise densities of the two detectors and γ is the normalized overlap reduction function, characterizing the loss of sensitivity due to the separation and the relative orientation of the detectors. We use the advanced LIGO sensitivity as an example of the second generation, the Einstein Telescope as an example of the third generation, and the LIGO Hanford/Livingston pair (H1-L1) as an example of separated detectors. For separated detectors the signal to noise ratio (S/N) is calculated between $10 - 150$ Hz and for co-aligned and coincident detectors, between $10 - 500$ Hz. We assume an observation time of $T = 3$ yr and detection threshold of $S/N = 1$ and $S/N = 5$.

5.2. magnetars

We investigate the constraints on the mean value of the effective external magnetic field B_{eff} and the deformation parameter β, for the *canonical model* with ms initial periods (dynamo process). Fig. 3 shows the detection limit in the plane $B_{eff} - \beta$ for advanced and third generation co-aligned and coincident detectors and for thresholds $S/N = 1$ and 5. At least with the third generation, we should be able to exclude the highest possible values of the magnetic field ($B_{\rm eff} > 10^{16}G$) and models with type II superconducting interior or with counter rotating electric currents. We could also put constraints on the internal toroidal component of the magnetic field B_t. If there is no detection, we should be able to confirm or rule out models for which the spindown is dominated by GW emission, for instance with $B_t >> B$ [40], which give $S/N \sim 2$ with advanced detectors and $S/N \sim 23$ with the third generation. With the first generation of detectors, unfortunately, it won't be possible to say anything, since we are well below the detection threshold, even for the most optimistic case when the spindown of the star is due to GW emission only.

5.3. Double neutron star coalescence

We use the model of section 4 to investigate the constraints on the fractions f_b and β_{ns}, or equivalently on the galactic coalescence rate R_{mw} (Table 1), given by statistical studies and source modeling in the range $10^{-4} - 10^{-6}$ yr^{-1}, more likely around 10^{-5} yr^{-1} [47, 42, 48]. With advanced coaligned and coincident detectors, we should be able to exclude the most optimistic predictions. It would become extremely interesting with the third generation, since we expect to reach the actual theoretical expectations with separated detectors and get very close to the lower limit with co-aligned and coincident detectors. If there is no detection with the third generation, we may have to review our models of binary evolution.

6. Conclusions

In this article, we reviewed the spectral and statistical properties of astrophysical backgrounds and presented two promising models for ground based detectors, as well as the constraints one can expect to put on the source parameters with the next generation of detectors. We showed that the energy density of astrophysical backgrounds is characterized by an increase at low frequencies (usually a power law), a maximum and a cutoff, at the maximum emission frequency in the source frame. For most of our models the peak occurs at kHz frequencies, where the sensitivity of pairs of separated detectors drops significantly. The best strategy may be to use co-aligned and coincident detectors such as the two LIGO Hanford interferometers; the issue is the presence of correlated noise, but new techniques are under development in the LIGO collaboration which should allow to use this pair in the near future [51]. On the other hand, the stochastic background may result in a popcorn noise or may be anisotropic at close redshifts, but

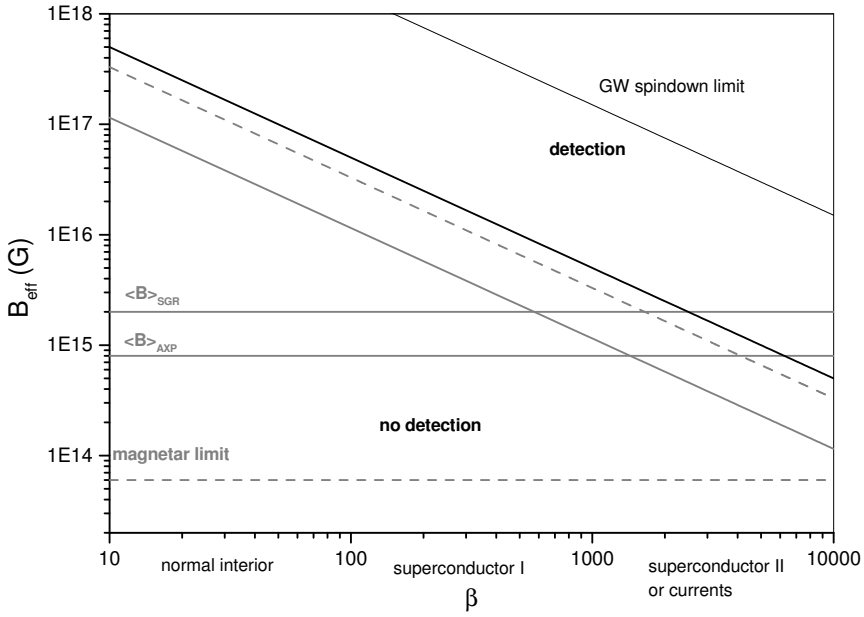

Figure 3. magnetars: constraints on the dipole external magnetic field $B_{\rm eff}$ and the distortion parameter β with co-aligned and coincident detectors and integration time $T = 3$ yr. The black continuous line corresponds to advanced detectors and a detection threshold $S/N = 1$, the light grey lines to 3rd generation detectors and $S/N = 1$ (continuous) and $S/N = 5$ (dashed). The grey continuous line shows the limit above which the spindown is almost purely gravitational and corresponds to $S/N \sim 2$ with advanced detectors and $S/N \sim 23$ with the third generation. The average values of $B_{\rm eff}$ for observed AXPs and SGRs as well as the magnetar limit, are also plotted for comparison.

	$(S/N)^{-1} f_b \beta_{ns}$	$(S/N)^{-1} R_{mw}$ yr^{-1}	R_{mw} yr$^{-1}(S/N = 5)$
inital (HL)	138.3	1.3	6.6
initial (c-co)	1.55	0.015	0.074
Ad (HL)	0.047	4.5×10^{-4}	0.0022
Ad (c-co)	0.0025	2.4×10^{-5}	1.2×10^{-4}
3rd (HL)	4.5×10^{-4}	4.3×10^{-6}	2.2×10^{-5}
3rd (c-co)	1.6×10^{-4}	1.5×10^{-6}	7.5×10^{-6}

Table 1. Constraints on the product $f_b \beta_{ns}$ and on the galactic coalescence rate R_{mw} of double neutron stars for different generation of detectors, for an integration time $T = 3$ yr and detection thresholds $S/N = 1$ (column 1 and 2) and $S/N = 5$ (third column). HL indicates a pair of detectors separated such as the LIGO Hanford-Livingston pair, and c-co a pair of co-aligned and coincident detectors. One can obtain the constraints for any detection threshold from columns 1 and 2 by multiplying the values given in column 1 and 2 ($S/N = 1$) by the S/N. Column 3 corresponds to $S/N = 5$)

again adequate detection strategies are also under investigation [52, 53]. We showed that we could already obtain interesting astrophysical results on simple models with advanced and third generation detectors, such as upper limits on the magnetic field or the ellipticity of magnetars or the coalescence rate of compact binaries. On the other hand we expect to be able to rule out or confirm some extreme models such as pure GW spindown in magnetars. Work is currently in progress to investigate a larger range of models and parameters and it will be reported in a future paper. What is particularly interesting with stochastic backgrounds, is that we can put constraints on the mean value of the population, and not just on some particular sources that may be in the tail of the probability distributions of the ellipticity or the magnetic field.

[1] Grishchuk L.P., Lipunov V.M., Postnov K.A., Prokhorov M.E. and Sathyaprakash B.S., 2001, Physics-Uspekhi, 44, 1 1993, CQG, 10, 2449
[2] Maggiore M., 2000, PhR, 331, 283
[3] Blair D. and Ju L., 1996, MNRAS, 283, 648
[4] Coward D., Burman R.R. and Blair D., 2001, MNRAS, 324, 1015
[5] Howell E., Coward D., Burman R. , Blair D. and Gilmore J., 2004, MNRAS, 351, 1237
[6] Buonanno A., Sigl G., Raffelt G.G., Janka H. T. and Mueller E. 2005, PRD, 72, 084001
[7] Ferrari V., Matarrese S., Schneider R., 1999, MNRAS, 303, 258
[8] de Araujo J.C.N., Miranda O.D. and Aguiar O.D., 2000, Nu.Ph.S., 80, 7
[9] de Araujo J.C.N., Miranda O.D. and Aguiar O.D., 2002a, CQG, 19, 1335
[10] de Araujo J.C.N., Miranda O.D., Oswaldo D. and Aguiar O.D., 2002b, MNRAS, 2002, 330, 651
[11] de Araujo J.C.N., Miranda O.D. and Aguiar O.D., 2004, MNRAS, 348, 1373
[12] Owen B.J., Lindblom L., Cutler C., Schutz B.F., Vecchio A., Andersson N., 1998, PRD, 58, 084020
[13] Ferrari V., Matarrese S., Schneider R., 1999b, MNRAS 303, 258
[14] Sigl G., 2006, JCAP, 04, 2
[15] Regimbau T. and de Freitas Pacheco J. A. 2006, ApJ,642, 455
[16] Regimbau T. and Chauvineaux B., 2007, CQG 24 627
[17] Regimbau T. and de Freitas Pacheco J. A., 2001, A&A, 376, 381
[18] Regimbau T. and de Freitas Pacheco J. A., 2006, A&A, 447, 1
[19] Ignatiev V.B. Kuranov A.G. Postnov K.A. and Prokhorov M.E., 2001, MNRAS, 327, 531
[20] Schneider R., Ferrari V., Matarrese S. and Potergies Zwart S.F., 2001, MNRAS, 324, 797
[21] Farmer A.J. and Phinney E.S., 2002, AAS, 34, 1225
[22] Cooray A., 2004 MNRAS, 354, 25
[23] Barack L. and Cutler C., 2004, PRD, 70, 122002
[24] Schnittman, J., Sigl G., Buonanno A., 2006, AIPC, 873, 437
[25] Rao S.M., Turnshek D.A. and Nestor D.B., 2006, ApJ 636, 610
[26] Perlmutter S. et al., 1999, ApJ, 517, 565
[27] Spergel D.N. et al. 2003, ApJS, 148, 175
[28] Hopkins A.M., Beacom J., 2006, ApJ, in press (asto-ph/0601463)
[29] Allen B., and Romano J., 1999, PRD, 59, 10
[30] Arnaud, N., et al., 1999, PRD, 59, 082002
[31] Pradier, T. et al., 2001, PRD, 63, 042002
[32] Drasco S., Flanagan E., 2003, PRD, 67, 8
[33] Coward D. and Burman R.R. 2005, MNRAS, 361, 362
[34] Duncan R. and Thompson C., 1992, ApJL, 392, 9
[35] Thompson C. and Duncan R., 1993, ApJ, 403, 194
[36] Kouveliotou et al., 1998, Nature, 393, 235
[37] Bonazzola S. and Gourgoulhon E., 1996, A&A, 312, 675
[38] Konno K., Obata T. and Kojima Y. 2000, A&A, 356, 234

[39] Cutler C. , 2002, PRD, 66, 084025
[40] Stella L. et al., 2005, ApJ, 634, 165
[41] Sathyaprakash B.S., gr-qc/0012014
[42] de Freitas Pacheco J.A., Regimbau T., Spallici A. and Vincent S. 2006, IJMPD, 15, 235
[43] Ando S., 2004, JCAP, 0406, 007
[44] OShaughnessy et al., astro-ph/07064139
[45] Belczynski et al., 2006, ApJ, 648, 1110
[46] Nagamine K., 2006, ApJ, 653, 881
[47] Kim C. et al. astro-ph/0405564
[48] Belczynski K., astro-ph/0612032
[49] Evans C.R., Iben I. and Smarr L., 1987, ApJ, 323, 129
[50] Coward D. and Regimbau T., 2006, New Astronomy Reviews, 50, 461
[51] Fotopoulos N., gr-qc/08013429
[52] Ballmer S., 2006, CQG, 23, S179
[53] Mitra S., Dhurandhar S., Souradeep T., Lazzarini A., Mandic V. and Bose S., 2008, PRD, 77, 042002